

Theoretical study on magnetic ground state in the layered perovskite SrCeCoO₄

ZHANG XIU'E*, KANG YONGGANG

Institute of Disaster Prevention, Sanhe Hebei, China, 065201

By using the unrestricted Hartree-Fock approximation and the real-space recursion method, we have investigated various magnetic structures in an enlarged double cell of layered perovskite SrCeCoO₄. These include the low-spin state ($t_{2g}^6 e_g^1$), high-spin state ($t_{2g}^5 e_g^2$), as well as all combinations among the two states. Our results show that the magnetic ground state mainly depends on the competition between the crystal field strength Dq and Hund's coupling j . For a fixed j the magnetic ground state is the high-spin antiferromagnetically ordered state.

(Received October 5, 2013; accepted May 15, 2014)

Keywords: Recursion method, Hartree-Fock approximation, Density of state, Layered perovskite, Spin state, Magnetic ground state

1. Introduction

Spin state is an important topic for many cobaltates, and it strongly affects or even determines their magnetic, electric, transport properties, and so on [1-6]. It can be a low spin (LS), a high spin (HS), or even an intermediate spin state (IS). This stems from a subtle interplay among the crystal field, Hund exchange, multiplet effect, spin-orbit coupling, and band hybridization.

In recent years, there are a lot of experimental and theoretically works have been done about the layered perovskite system, for example La_{2-x}Sr_xCoO₄, Sr₂CoO₄, and LaSrCoO₄ [7-12]. While few experiment works have been done about the magnetic property of the electron-doped layered perovskite Sr_{2-x}Ce_xCoO₄. In order to better understand the magnetic and electronic properties of the doped system, it is worthwhile to first investigate the half doped compound SrCeCoO₄. It surely helps us to resolve the complex doped situation if a clear physical picture on magnetic structure emerges from layered SrCeCoO₄. Thus we will study in this paper various magnetic states in an enlarged double cell of SrCeCoO₄. In addition to the low-spin state (LS, $t_{2g}^6 e_g^1$), and high-spin state (HS, $t_{2g}^5 e_g^2$), we also consider all possible spin and

charge ordered combinations among the two states. Note that the definitions of the two states are different from the ones in the other end member LaSrCoO₄ because the former has one electron more than the latter. The calculation is performed within the unrestricted Hartree-Fock approximation on a realistic perovskite-type lattice model and the self-consistent solutions are obtained using the iteration method. The band-structure parameters are deduced from the cluster model analysis of the photoemission spectra [13,14]. To compare the relative stability of the various states, we compute their energies as functions of the crystal-field strength $10Dq$ and Hund's coupling j since the phase diagram mainly depends on the competition between these two parameters. Our results show that for a fixed exchange coupling j , the ground state of the system is high-spin antiferromagnetically ordered state (HS-HS-AFM).

2. Theoretical formalism

Since the rare earth elements form paramagnetic ions which contribute little to the density of states at the Fermi energy, only transition metal 3d orbitals and oxygen 2p

orbitals play important roles. Thus we adopt the general multiband d - p model Hamiltonian [15]

$$\begin{aligned}
H = & \sum_{im\sigma} \hat{a}_{im\sigma} \mathcal{E}_{dm}^0 d_{im\sigma}^+ d_{im\sigma} + \sum_{jn\sigma} \hat{a}_{jn\sigma} \varepsilon_p p_{jn\sigma}^+ p_{jn\sigma} + \\
& \sum_{ijmn\sigma} \hat{a}_{ijmn\sigma} (t_{ij}^{mn} d_{im\sigma}^+ p_{jn\sigma} + H.c.) + \\
& \sum_{ijnm'\sigma} \hat{a}_{ijnm'\sigma} (t_{ij}^{m'n'} p_{jn'\sigma}^+ p_{im'\sigma} + H.c.) + \\
& \sum_{im} \hat{a}_{im} u d_{im}^+ d_{im}^- + \\
& \frac{1}{2} \tilde{u} \sum_{im'm'\sigma\sigma'} \hat{a}_{im'm'\sigma\sigma'} d_{im\sigma}^+ d_{im'\sigma}^- d_{im'\sigma'}^+ d_{im\sigma'}^- + \\
& J_H \sum_{im\sigma\sigma'} \hat{a}_{im\sigma\sigma'} d_{im\sigma}^+ \sigma d_{im\sigma'} \cdot S_{im}^d
\end{aligned} \quad (1)$$

Where $d_{im\sigma}^-$ ($d_{im\sigma}^+$) and $p_{jn\sigma}^-$ ($p_{jn\sigma}^+$) denote the annihilation (creation) operators of an electron on a Co- d orbital at site i and an O- p orbital at site j respectively, and \mathcal{E}_{dm}^0 and ε_p are their corresponding on-site energies. m and n refer to the orbital index and σ denotes the spin. The crystal-field-splitting energy is included

in \mathcal{E}_{dm}^0 , i.e., $\mathcal{E}_d^0(t_{2g}) = \mathcal{E}_d^0 - 4Dq$, $\mathcal{E}_d^0(e_g) = \mathcal{E}_d^0 + 6Dq$,

where \mathcal{E}_{dm}^0 is the bare on-site energy of d orbital. t_{ij}^{mn} and $t_{ij}^{m'n'}$ are the nearest-neighbor hopping integrals for p - d and p - p , which are related to the Slater-Koster parameters ($pd\sigma$), ($pd\pi$), ($pp\sigma$), and ($pp\pi$)[16]. S_{im}^d is the total spin operator of a Co ion, extracting the one in orbital m . The parameter J_H is the Hund's coupling constant, $\tilde{u} = u - 5J_H/2$, where the parameter u is related to the multiplet averaged d - d Coulomb interaction U via $u = U + (20/9)J_H$.

In the unrestricted Hartree-Fock approximation, the Hamiltonian becomes linearized and reduces to

$$\begin{aligned}
H = & \sum_{im\sigma} \hat{a}_{im\sigma} \mathcal{E}_{dm}^0 d_{im\sigma}^+ d_{im\sigma} - \frac{J_H}{2} \sigma (\mu_t^d - \mu_m^d) \sum_{im\sigma} \hat{a}_{im\sigma} \tilde{u} (n_t^d - n_m^d) d_{im\sigma}^+ d_{im\sigma} \\
& + \sum_{jn\sigma} \hat{a}_{jn\sigma} \varepsilon_p p_{jn\sigma}^+ p_{jn\sigma} + \sum_{ijmn\sigma} \hat{a}_{ijmn\sigma} (t_{ij}^{mn} d_{im\sigma}^+ p_{jn\sigma} + H.c.) \\
& + \sum_{ijnm'\sigma} \hat{a}_{ijnm'\sigma} (t_{ij}^{m'n'} p_{jn'\sigma}^+ p_{im'\sigma} + H.c.)
\end{aligned} \quad (2)$$

Here $n_{m\sigma}^d = \langle d_{m\sigma}^+ d_{m\sigma} \rangle$, $\mu_m^d = n_m^d - n_m^{-d}$, and n_t^d and μ_t^d are the total electron numbers and magnetization of the Co d orbitals. For the tight-binding Hamiltonian (2), the density of states can be easily calculated using the real-space recursion method [17] and the Green's function is written as

$$G_{m\sigma}^0(\omega) = \frac{b_0^2}{\omega - a_0 - \frac{b_1^2}{\omega - a_1 - \frac{b_2^2}{\omega - a_2 - \frac{b_3^2}{\omega - a_3 - \dots}}}} \quad (3)$$

The recursion coefficients a_i and b_i are obtained from the tridiagonalization of the tight-binding Hamiltonian matrix for a given starting orbital. The multiband terminator [18] is chosen to close the continuous fractional. To study the spin state transition in SrCeCoO₄, we have considered various ordered states of an enlarged double cell of SrCeCoO₄. We have computed 25 levels for each of the 68 independent orbital; the results are checked for different levels and better than 5meV in energy accuracy is secured. The whole procedure is iterated self-consistently until convergence and the density of states is obtained by $\rho_{m\sigma}(\omega) = - (1/\pi) \text{Im} G_{m\sigma}(\omega)$. This allows us to calculate the electron numbers and magnetic moments, as well as the energies of various ordered states.

3. Numerical results and discussions

Since there have been relatively few studies on layered perovskite SrCeCoO₄, there are no direct experimental data on the band structure parameters, and thus these parameters have to be estimated from their

counterpart of LaCoO3[19,15], since the size of Co-O6 octahedron of SrCeCoO4 is essentially the same as that of LaCoO3[20]. As the Slater-Koster parameters approximately satisfy the scaling relation, they are taken as $(pd\sigma) = -2.0$ eV, $(pd\pi) = 0.922$ eV, $(pp\sigma) = 0.6$ eV, and $(pp\pi) = -0.15$ eV, respectively. The nearest-neighbor hopping integrals between the oxygens of neighboring layers can be obtained using the formula [21]

$V_{ll\phi n} = \eta_{ll\phi n} (\hbar^2 / md^2)$ with d denoting the interatomic distance, they are given $(pp\sigma) = 0.334$ eV, and $(pp\pi) = -0.084$ eV. The bare on-site energies of Co- d and O- p orbitals are taken as $\varepsilon_d^0 = 28.0$ eV and $\varepsilon_p = 0$ eV. The on-site Coulomb repulsion is $U = 5.0$ eV. The crystal-field splitting and Hund's coupling are set as $Dq = 0.14$ eV and $J_H = 0.90$ eV which is slightly larger than that in LaCoO₃ because the configuration of Co²⁺ in the ground state of La₂CoO₄ [22] is $t_{2g}^5 e_g^2$ (high-spin state) rather than $t_{2g}^6 e_g^1$ (low-spin state).

The lattice parameters of SrCeCoO4 with tetragonal symmetry are taken $a = 3.8097$ Å and $c = 12.4788$ Å from Ref. [23]. With the parameter set given above, we have investigated the electronic structures of LS, HS as well as all possible spin combinations among them. The stability of various states is analyzed for different Dq and j . Our results indicate that five magnetic structures with different spin-state are found to be metastable and the HS-HS-AFM state is the ground state. In the following, we discuss these states one by one.

The first state we considered is the LS state. As can be seen from the density of states presented in Fig. 1(a), this state corresponds to a poor metal, since the density of states at the Fermi energy is quite small and below the Fermi energy ($E_F=0$) is a broad Energy gap. The magnetic moment and occupancy of the d orbital are $0.97 \mu_B$ and 7.42, respectively. In fact, ferromagnetic LS state has rather higher energy in the states we studied, it cannot

become the ground state unless the Hund's coupling j is extremely large.

In comparison with the ferromagnetic LS state, the density of state of ferromagnetic HS state shown in Fig. 1(b) is even more broadly distributed since t_{2g} and e_g band splitted further because of the larger magnetic moment. The overall shape of the density of states is quite similar to the LS state except for a broad Energy gap lie in the Fermi level and a small peak above the E_F , so this state is an insulator. The magnetic moment of the HS state is $2.72 \mu_B$ and the occupancy of the d band is 7.26.

As displayed in Fig. 1(c), the density of states of LS-HS state has a broader band structures than that of LS state and the gross feature is very close to that of the HS state. The structures in the vicinity of E_F mainly stem from the t_{2g} band and the major part of the valence band comes from O- p orbitals. This state is a paramagnetic insulator since the Fermi energy lies within the gap. The occupancy of the Co d orbital is 7.48 for the LS site and 7.24 for the HS site; the magnetic moment is $1.07 \mu_B$ for the LS site and $2.72 \mu_B$ for the HS site.

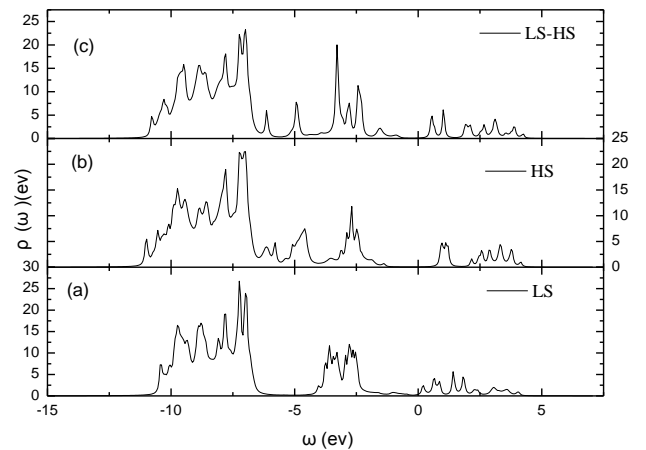


Fig. 1. The total density of states for (a) LS state, (b) HS state, and (c) LS-HS state for $J_H = 0.90$ eV and $Dq = 0.14$ eV. The other parameters are described in the text.

In addition to the translational invariant states discussed above, below we concentrate on the various

spin-ordered antiferromagnetic states in an enlarged double cell of SrCeCoO₄. The first spin state is the antiferromagnetically ordered LS (LS-LS-AFM) state as shown in Fig. 2(a), the main difference from the ferromagnetic LS state in Fig. 1(a) stems from the further splitted Co-*d* bands and the peaks become even sharper due to antiferromagnetic ordering. The LS-LS-AFM is a band insulator with a gap of the order of 2.05 eV. The electron occupancy and magnetic moment of Co-*d* are 7.43 and 0.88 μ_B , respectively.

The next spin state is the antiferromagnetically ordered HS-HS-AFM state plotted in Fig. 2(b), like most of the antiferromagnets at integer electron filling, this state is also a band insulator. But its energy gap is the broadest among the above states. The occupancy of the Co-*d* bands is 7.29 and the corresponding magnetic moment is 2.68 μ_B . As we will see later in this paper, this state is the ground state of the system with the lowest energy following crystal field strength *Dq* decrease.

The last antiferromagnetically ordered state is the LS-HS-AFM state presented in Fig. 2(c) which can be envisaged as a superposition between HS-HS-AFM and LS-LS-AFM. This state is also a band insulator, its band gap is more or less the same as that of LS-LS-AFM state. The occupancy of the Co-*d* orbital is 7.49 for the LS site and 7.27 for the HS site; the magnetic moment is 1.00 μ_B for the LS site and 2.69 μ_B for the HS site.

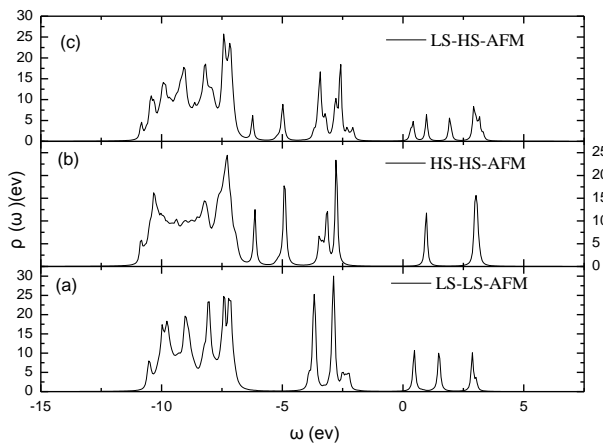


Fig. 2. The total density of states for (a) LS-LS-AFM state, (b) HS-HS-AFM state, and (c) LS-HS-AFM state. The parameters are the same as in Fig. 1.

In order to determine which spin structure will be the most probable candidate of the ground state of SrCeCoO₄, we have calculated energies per double cell of various states as functions of crystal-field splitting *Dq* and for two sets of Hund's coupling $J_H = 0.90$ eV and $J_H = 0.94$ eV.

It is shown in Fig. 3 that as crystal-field splitting *Dq* changes from 0.10 eV to 0.20 eV, only the HS-HS-AFM state can become the ground state of the system. We would like to point out that the energy diagram for different *j* looks the same except for a shift of the crossover points on *Dq*. Other structures we studied are energetically unfavorable in the relevant parameter region of the compound. Since Hund's coupling J_H and the crystal field strength *Dq* affect the energies in a correlated fashion. In the following, we are mainly interested in the magnetic ground state HS-HS-AFM state.

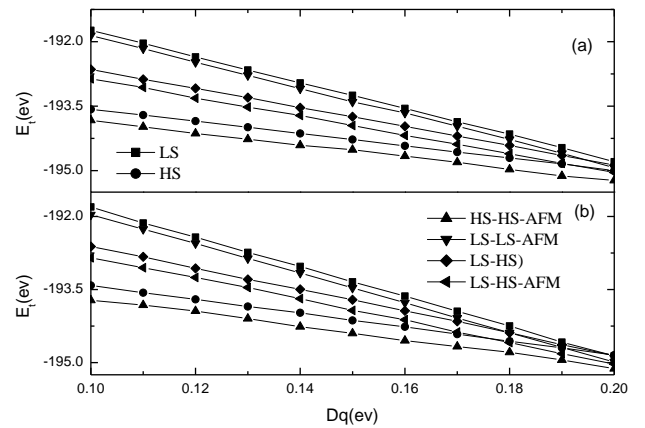


Fig. 3. The energies per double cell of the various spin states as a function of *Dq*; (a) $J_H = 0.94$ eV and (b) $J_H = 0.90$ eV. Other parameters are described in the text.

In order to better understand the magnetic properties of the ground states, we discuss the HS-HS-AFM state in more detail. The total density of states (TDOS) and the spin resolved partial densities of states (PDOS) are presented in Fig. 4. The TDOS shown in Fig. 4(a) and the PDOS for both O-*p* orbitals and Co-*d* orbitals are plotted in Figs. 4(b-d). The PDOS of Co-*d* (t_{2g}) and Co-*d* (e_g) are differentiated with solid and dotted lines in the middle panel. It is found that the density of states of the Co-*d* (t_{2g})

orbital is very localized near the Fermi energy and that of Co- $d(e_g)$ orbital is quite extended. For the total density of states, The first peak above the Fermi energy is contributed by Co(1)- $d(t_{2g})$ and Co(2)- $d(t_{2g})$ orbital while the top peak just above the Fermi energy result from the Co(1)- $d(e_g)$ and Co(2)- $d(e_g)$ orbitals; and the first peak below the Fermi energy is contributed by Co- $d(t_{2g})$ orbital while below the Fermi energy the main body of the valence band is mainly of O- p character.

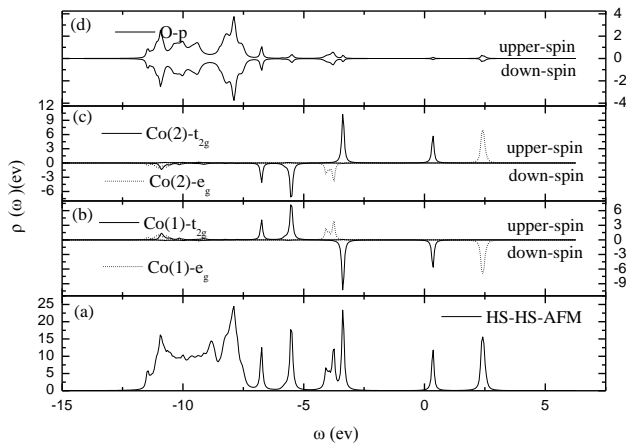


Fig. 4. The density of states per double cell of the HS-HS-AFM state for $Dq = 0.14$ eV. (a) Total DOS; (b) PDOS of Co(1)- d ; (c) PDOS of Co(2)- d ; (d) PDOS of O- p . Other parameters are described in the text.

4. Conclusion

In this paper, we have studied various spin ordered structures in an enlarged double cell of layered perovskite SrCeCoO₄ using the unrestricted Hartree-Fock approximation of the multiband $d-p$ model, six convergent states are analyzed in detail and the phase diagram is obtained as functions of the crystal-field splitting and Hund's coupling. It is found that the HS-HS-AFM state is the ground state of the charge-ordered system.

Acknowledgments

This work is supported by Teachers' Scientific Research Fund of China Earthquake Administration (20120121). We are very grateful to Professor Aimin Sun for kindly offering his advice.

References

[1] R. F. Klie, J. C. Zheng, Y. Zhu, M. Varela, J. Wu, C. Leighton, Phys. Rev. Lett **99**, 047203 (2007).

- [2] S. K. Pandey, A. Kumar, S. Patil, V. R. R. Medicherla, R. S. Singh, K. Maiti, D. Prabhakaran, A. T. Boothroyd, A. V. Pimpale, Phys. Rev. B **77**, 045123 (2008).
- [3] J. M. Rondinelli, N. A. Spaldin, Phys. Rev. B **79**, 054409 (2009).
- [4] N. Sundaram, Y. Jiang, I. E. Anderson, D. P. Belanger, C. H. Booth, F. Bridges, J. F. Mitchell, Th. Proffen, H. Zheng, Phys. Rev. Lett **102**, 026401 (2009).
- [5] K. Knížek, Z. Jirák, J. Hejtmánek, P. Novák, W. Ku, Phys. Rev. B **79**, 014430 (2009).
- [6] H. Luetkens, M. Stingaciu, Yu. G. Pashkevich, K. Conder, E. Pomjakushina, A. A. Gusev, K. V. Lamonova, P. Lemmens, H.-H. Klauss, Phys. Rev. Lett **101**, 017601 (2008).
- [7] J. Wang, W. Zhang, D. Y. Xing, Phys. Rev. B **62**, 14140 (2000); J. Wang, Y. C. Tao, W. Zhang, D. Y. Xing, J. Phys.: Condens. Matter **12**, 7425 (2000).
- [8] S. K. Pandey, Phys. Rev. B **81**, 035114 (2010).
- [9] K.W. Lee, W. E. Pickett, Phys. Rev. B **73**, 174428 (2006).
- [10] H. Wu, Phys. Rev. B **81**, 115127 (2010).
- [11] H. Wu, T. Burnus, Phys. Rev. B **80**, 081105 (2009).
- [12] A. V. Chichev, M. Dlouhá, S. Vratilav, K. Knížek, J. Hejtmánek, M. Maryško, M. Veverka, Z. Jirák, N. O. Golosova, D. P. Kozlenko, B. N. Savenko, Phys. Rev. B **74**, 134414 (2006).
- [13] T. Saitoh, T. Mizokawa, A. Fujimori, M. Abbate, Y. Takeda, M. Takano, Phys. Rev. B **55**, 4257 (1997).
- [14] A. Chainani, M. Mathew, D. D. Sarma, Phys. Rev. B **46**, 9976 (1992).
- [15] T. Mizokawa, A. Fujimori, Phys. Rev. B **53**, R4201 (1996); Phys. Rev. B **54**, 5368 (1996); Phys. Rev. B **51**, 12880 (1995).
- [16] J. C. Slater, G. F. Koster, Phys. Rev **94**, 1498 (1954).
- [17] V. Heine, R. Haydock, M. J. Kelly, in Solid State Physics: Advances in Research and Applications, edited by H. Ehrenreich, F. Seitz, D. Turnbull (Academic, New York, 1980), p. 215.
- [18] R. Haydock, C. M. M. Nex, J. Phys. C **17**, 4783 (1984).
- [19] M. Zhuang, W. Zhang, N. Ming, Phys. Rev. B **57**, 10705 (1998).
- [20] T. Matsuura, T. Tabuchi, J. Mizusaki, S. Yamauchi, K. Fueki, J. Phys. Chem. Solids **49**, 1403 (1988).
- [21] W. A. Harrison, in Electronic Structure and the Properties of Solids (W. H. Freeman and Company, San Francisco, 1980) p. 27.
- [22] K. Yamada, M. Matsuda, Y. Endoh, B. Keimer, R. J. Birgeneau, S. Onodera, J. Mizusaki, T. Matsuura, G. Shirane, Phys. Rev. B **39**, 2336 (1989).
- [23] Y. Moritomo, K. Higashi, K. Matsuda, A. Nakamura, Phys. Rev. B **55**, R14725 (1997).

*Corresponding author: zhangxiue2005@163.com